GROUND TRUTH EVENTS FROM REGIONAL SEISMIC NETWORKS IN NORTHEASTERN AFRICA

Richard A. Brazier[1], Yongcheol Park[1], Andrew A. Nyblade[1], and Michael E. Pasyanos[2]

Penn State University[1] and Lawrence Livermore National Laboratory[2]

Sponsored by National Nuclear Security Administration
Office of Nonproliferation Research and Engineering
Office of Defense Nuclear Nonproliferation

Contract No. DE-FC03-02SF22500[1] and W-7405-ENG-36[2]

ABSTRACT

Determining accurate seismic locations, with representative uncertainty estimates, is of fundamental importance to ground-based nuclear explosion monitoring. This project is developing a catalog of reference events (ground truth (GT)), in the northeast African area of interest, where reference event coverage is exceptionally poor because of the limited station coverage by historic networks. The results of this project will enable the seismic monitoring community to enhance their operational capability to monitor for nuclear tests in north Africa and the Middle East by increasing their ability to accurately locate and identify seismic events in these regions.

The collection of ground truth events for northeastern Africa is being achieved using state-of-the-art event location methods applied to broadband seismic data from regional PASSCAL networks in Ethiopia, Kenya and Tanzania, as well as to broadband data from primary and auxiliary International Monitoring System (IMS) stations in the region. The ground truth catalog is being assembled by determining origin time, focal mechanism and hypocenters for many events that lie within close proximity of recording stations or else are well recorded teleseismically.

Accurate event locations for fourteen M>3.5 events, in northeastern Africa, have been obtained thus far using data from the Tanzania Broadband Seismic Experiment and the Ethiopia Broadband Seismic Experiment. Focal mechanisms for most of these events have been obtained by modeling P and SH polarities and amplitude ratios in a grid search method. Epicenters have been constrained by using P and S arrival times. Focal depths have been constrained by waveform modeling of regional and local depth phases. Most of the earthquakes occur on either the western or eastern branch of the East African Rift, and the mechanisms obtained are all normal or strike-slip. Preliminary epicentral locations for several hundred additional local and near-regional earthquakes have been obtained for Ethiopia using P arrival times.

The Bayesian kriging method is being used with the well located events to construct regional travel-time correction surfaces for northern Africa. To improve further our capabilities to accurately locate events in this part of the world, we are also using surface wave data to construct new velocity models of the crust and upper mantle. Group velocity measurements from many thousand station event pairs ranging from 15-60 second periods for Rayleigh and Love waves have been measured, and these measurements have been inverted to produce group velocity maps of eastern Africa.

OBJECTIVE

Introduction

Determining accurate seismic locations with representative uncertainty estimates is of fundamental importance to ground-based nuclear explosion monitoring. In this project, we are developing a catalog of reference events (GT) in the northeast Africa where reference event coverage is exceptionally poor due to the limited station coverage by historic networks. We are developing a catalog of accurately located hypocenters within a range of GT levels, origin times, and focal mechanisms for several tens of earthquakes with magnitudes > 3. The catalog will enable the seismic monitoring community to enhance their operational capability to monitor for nuclear tests in North Africa and the Middle East by increasing their ability to accurately locate and identify seismic events in these regions.

Earthquakes in northeastern Africa provide a principal source of ground truth for north Africa and the Middle East. The earthquakes of interest are associated with the northern and central portions of the East African Rift System (Figure 1). Since there are very few earthquakes within North Africa proper or within large parts of the Middle East that can be used to develop a set of ground truth, naturally occurring events in northeastern Africa take on an added importance for improving monitoring capabilities in the region for the Comprehensive Nuclear-Test-Ban Treaty (CTBT).

The development of GT for north Africa and the Middle East has in the past been limited not only by the lack of appreciable seismicity but also by a dearth of seismic stations throughout most of Africa. This situation is now changing. We operated regional seismic networks in Ethiopia and Kenya comprised of 27 and 11 broadband stations, respectively, between 2000 and 2002, and several years ago (1994-1995) we operated a similar network of 20 broadband seismic stations in Tanzania. The broadband waveforms recorded by these networks, together with waveforms from primary and auxiliary IMS stations in the region, provide a rich data set that can be used to accurately locate earthquakes and determine their origin times and source mechanisms.

The GT catalog is being assembled by (1) determining origin time, focal mechanism and hypocenters for many events that lie within close proximity of recording stations or else are well recorded teleseismically; (2) using these events to construct regional travel time correction surfaces using a Bayesian kriging technique, and (3) using the travel time correction surfaces to obtain origin times and epicenters for numerous other events. Robust estimates of the uncertainties in the locations and origin times will also be determined.

Here we present improved locations for 11 events within Tanzania with M>4 and 3 events from Ethiopia with M >3.5 constrained by P and S arrival times and pPn, sPn, and Pmp depth phases recorded by the regional broadband networks in Tanzania and Ethiopia. We begin by providing background information about the geology of the region and on the broadband seismic experiments. This is followed by a discussion of our ongoing work of our event locations and uncertainties including a group velocity tomography for eastern Africa and travel time correction surfaces to improve locations and determine new locations.

Background Information

The locations of the broadband seismic experiments, together with the geology and topography of east Africa, are shown in Figure 1. The geology of the region is comprised of an Archean craton (the Tanzania craton, Figure 1) surrounded by Proterozoic mobile belts. The rift faults of the Cenozoic East African Rift System have developed mainly within the Proterozoic mobile belts, forming a rift system that begins with the Main Ethiopian Rift intersecting the Red Sea and the Gulf of Aden at the Afar triple junction continuing southwest through Kenya and splitting into two branches (western rift and eastern rift) around the Tanzanian craton.

The broadband seismic experiment in Tanzania was conducted in 1994 and 1995 and consisted of 20 seismic stations deployed for a year in two skewed arrays; one oriented more or less east-west, and the other northeast-southwest. The experiment was designed so that structure beneath the Archean Tanzania craton and the terminus of the eastern rift in northern Tanzania could be imaged with seismic data from local, regional and teleseismic earthquakes. Information about the station configuration, recording parameters and other details of the field deployment has been reported by Nyblade et al. (1996).

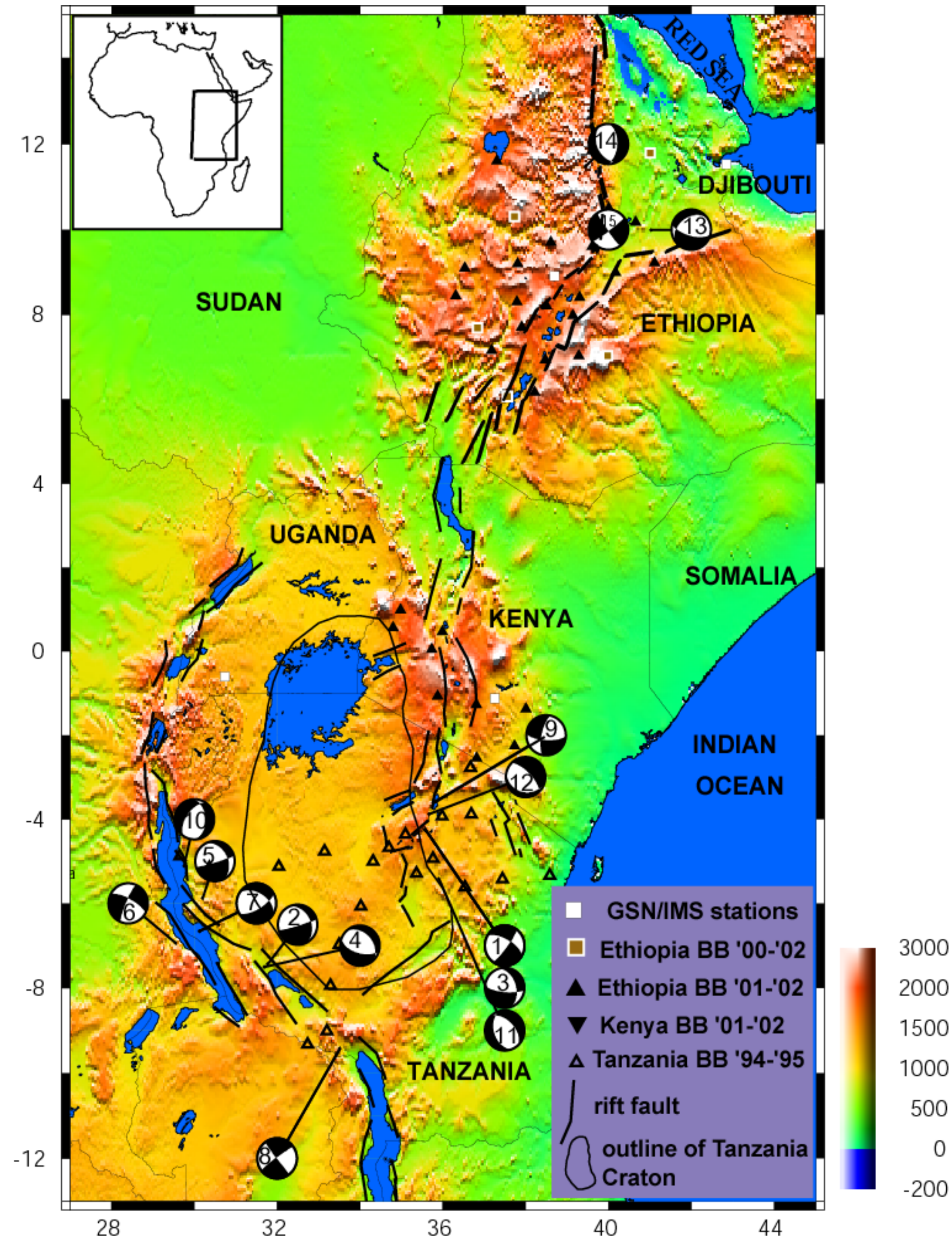

Figure 1. Topographic map of east Africa showing the Ethiopian and east African plateaus (regions with >1,000 m elevation), the outline of the Archean Tanzania craton, the major rift faults of the East African Rift System, focal mechanisms for our events, and the location of broadband seismic stations.

In the other broadband seismic experiments, seismic stations consisting of broadband sensors, 24-bit data loggers, 4 Gbyte hard disks, and GPS clocks were deployed in regions of Ethiopia and Kenya safe for traveling (Figure 1). The stations were spaced 50 to 200 km apart and were located to optimize the recording of teleseismic body and surface waves that sample upper mantle structure beneath the eastern rift. For east Africa, the major source regions for teleseismic earthquakes are the Hindu Kush/Pamir region to the northeast and the Fiji/Tonga subduction zones to the east. Additional criteria used for site selection included access to bedrock, security, and year-round road conditions.

Installation of the Ethiopian stations was completed in two phases. During March 2000, five stations were installed around the periphery of the network, and then one year later (March 2001) an additional 20 stations were installed to densify the network (Figure 1). All 25 stations were removed from the field in March 2002. Installation of the Kenyan stations took place during July and August 2001, and all 10 of the stations were removed in July 2002. Two data streams were recorded, a 1 sample/sec continuous stream and a 20 sample/sec continuous stream, yielding a data volume of 21 Mbytes per station per day. Data recovery for the Ethiopian stations was nearly 90%, and it was about 70% for the Kenyan stations.

EVENT LOCATIONS

Event locations have been obtained for several events in Tanzania with magnitudes $\geq$ 4 and in Ethiopia with magnitudes > 3.5 that were well recorded by the Tanzania and Ethiopia regional networks. The locations were obtained using P and S arrival times, a regional velocity model for the crust and upper mantle constrained by a number of previous studies, and the event location code HYPOELLIPSE (Lahr, 1993). The P and S onset times were individually handpicked to within 0.1 seconds. The velocity models in Table 1 were used in the event location code for each respective region. Crust and uppermost mantle in east Africa has been studied in detail by many authors using refraction surveys, receiver functions, surface waves, regional waveforms and Pn tomography. From these studies, it is clear that Tanzania's crustal and uppermost mantle structure is fairly uniform in the Precambrian terrains away from the rift valleys proper (Last et al., 1997; Brazier et al., 2000; Nyblade, 2002; Langston et al., 2002; Fuchs et al. 1997 and references therein). Only minor differences in crustal thickness (2-5 km), mean crustal velocity (0.1-0.2 km/s), and uppermost mantle P velocities (0.1 – 0.2 km/s) are found between the various stations of the Tanzania network, and these differences introduce very small uncertainties in the event locations.

Table 1. Crust and uppermost mantle seismic structure for Tanzania and Ethiopia, east Africa.

	V1 (km/s)	V2 (km/s)	Poisson's Ratio	Moho Depth (km)	Mean crustal Vp (km/s)	Pn (km/s)
Tanzania	5.84	7.09	0.25	38	6.5	8.3
Ethiopia	6.2	6.99	0.25	44	6.4	8.0

V1= uppermost crustal velocity; V2=lowermost crustal velocity

Table 2 summarizes the event origin times and locations, and the uncertainties associated with the locations. All of the events are well recorded on at least 11 stations in Tanzania 6 in Ethiopia. A number of the events are within a few tens of kilometers of a station and none are more than a few hundred kilometers from a station. The magnitude estimates for these events comes from using the maximum P wave amplitude within the first five seconds and the local magnitude scale for east Africa determined by Langston et al. (1998). Standard statistical measures at the 68% confidence interval in the error ellipse indicate that the hypocenters appear to be constrained to within a few kilometers. However, a detailed study of several of these events using regional waveform modeling (Langston et al., 2002) indicates that while the P and S arrival times do a fairly good job at constraining epicentral location, they do not provide tight constraints on source depth. Source depth for the events studied by Langston et al. (2002) is shown in Table 2. The source depth obtained from the P and S arrival times for these events differed from the source depths in Table 2 by ten or more kilometers.

Focal mechanisms have been determined using polarities and amplitude ratios of local and regional P and S phases using the grid-search technique by Snoke (1984) and are plotted in Figure 1 and are listed in Table 3. The focal mechanisms are then used with a wavenumber integration algorithm (Kennett, 1983) to compute full synthetic seismograms for several stations at several depths. The synthetics are compared against the data and regional depth phases such as pPn, sPn and PmP can be used to constrain the source depths. In Figure 2 we show the P wave train from the vertical component for an event from Tanzania. These traces are reduced to the Pn velocity. Focal depth is determined by finding the depth at which the best alignment occurs between the data and synthetics. Fixing this depth and relocating using hypoellipse gives a more accurate location overall.

For comparison, we also show in Table 2 the locations and origin times for several of the events taken from the International Seismological Centre (ISC) catalog, our earlier results without depth determination, and two locations including stations outside the networks. The comparison shows discrepancies in origin times of several seconds in most cases, and differences in event location of many tens of kilometers for some events. In addition, no catalog listings were found for several of the events.

Table 2. Locations for earthquakes in east Africa with M > 4 from July 94 June 95 recorded by the Tanzania Broadband Seismic Experiment and the Ethiopia Regional Network from April 2000 to March 2002.

Event:source	yr:mo:day:hr:min:sec	Lat.	Lon.	Dep	M	N	Gap	RMS	Smaj	Az	Smin	Sez
1:Traveltimes	94:07:20:11:32:04.30	-4.080	35.440	42	4.5	19	141	0.44	0.25	-106	0.45	1.7
1:ISC	94:07:20:11:31:58.49	-4.171	35.185	0	3.8			1.26	10.4	90	6.6	
1:Fixed Depth	94:07:20:11:32:04.09	-4.225	35.585	29^{+}	4.5	19	133	1.52	0.25	-106	0.40	0.47
2: Traveltimes	94:08:17:03:23:34.98	-4.513	35.277	17	3.7	20	76	0.70	0.22	-104	0.33	.42
2: Fixed Depth	94:08:17:03:23:32.68	-4.448	35.585	13	3.7	20	18	4.05	0.22	-105	0.31	.52
3: Fixed Depth	94:08:18:00:45:48.80	-7.440	31.770	25^{*}	5.9^{+}	17	167	1.77	0.35	-34	0.48	2^{*}
3: ISC	94:08:18:00:45:52.70	-7.650	31.830	25	5.9			0.69	2.20	90	2.20	
4: Traveltimes	94:09:05:04:08:56.04	-7.508	31.700	?	4.1	15	174	0.43	0.41	-59	0.70	?
4: ISC	94:09:05:04:08:50.41	-7.738	30.882	4	4.6			1.38	10.9	90	6.3	
4: Fixed Depth	94:09:05:04:08:54.83	-7.502	31.700	15^{+}	4.1	18	174	0.54	0.38	-50	0.55	2^{*}
5: Traveltimes	94:09:30:01:36:53.14	-5.920	29.890	26	4.5	16	229	1.13	0.55	-40	1.18	1.4
5: ISC	94:09:30:01:36:47.62	-8.426	37.261	0	4.4			1.78	15.6	90	8.6	
6: Traveltimes	94:11:12:12:18:00.00	-6.950	29.920	30^{*}	5.3	16	179	0.55	0.42	-24	0.89	2^{*}
6: ISC	94:11:12:12:18:01.33	-6.777	29.821	22	4.6			1.05	6.3	90	4.5	
6: Fixed Depth	94:11:12:12:18:00.88	-6.708	30.111	18^{+}	5.3	16	179	0.95	0.39	-26	0.74	2^{+}
6: Fixed Depth +	94:11:12:12:17:57.73	-6.939	29.552	18^{+}	5.3	23	94	2.13	0.31	-40	0.36	2^{+}
7: Traveltimes	94:11:12:20:16:59.37	-6.617	30.016	?	4.7	17	223	0.88	0.45	-33	0.96	?
7: ISC	94:11:12:20:16:49.66	-6.834	29.946	0	4.6			1.15	8.4	90	5.5	
7: Traveltimes	94:11:12:20:16:58.19	-6.652	30.135	8	4.7	17	211	1.29	0.39	-26	0.73	2*
8: Traveltimes	94:11:16:01:08:11.20	-9.070	33.330	8^{*}	4.5	17	193	0.80	0.48	-129	0.66	2^{*}
8: ISC	94:11:16:01:08:09.07	-9.179	33.273	10	5.0			1.64	7.8	90	6.8	
8: Fixed Depth	94:11:16:01:08:10:21	-9.145	33.454	7^{+}	4.5	17	204	0.86	0.51	-112	0.73	2^{+}
8: Fixed Depth +	94:11:16:01:08:05.78	-9.424	33.513	7^{+}	4.5	20	150	3.6	0.29	-52	0.54	0.97
9: Traveltimes	94:11:27:04:20:51.65	-3.568	35.827	30	4.0	15	213	0.51	0.36	-93	0.95	0.7
9: ISC	94:11:27:04:20:44.27	-3.954	35.722	10	4.0			0.12	22.4	90	10.1	
9: Fixed Depth	94:11:27:04:20:53.71	-4.084	35.828	11	4.0	15	146	2.28	0.29	-112	0.48	0.7
10: Traveltimes	94:12:25:04:25:27.44	-5.113	29.752	21	4.2	11	301	0.59	0.81	19	6.42	1.9
10: Fixed Depth	94:12:25:04:25:35.97	-5.173	30.580	29	4.2	11	150	1.48	0.67	22	4.98	2*
11: Traveltimes	95:01:29:00:23:35.02	-5.419	35.909	13	4.1	11	128	0.37	0.34	-107	0.51	1.0
11: Fixed Depth	95:01:29:00:23:33.29	-5.033	35.923	9	4.1	11	111	3.51	0.31	-111	0.53	1.04
12: Traveltimes	95:02:12:16:37:30.00	-3.960	35.830	32^{*}	4.5	20	?					2^{*}
12: Fixed Depth	95:02:12:16:37:33.85	-3.879	35.670	34^{+}	4.5	13	215	0.56	0.36		0.96	2^{+}
13: ISC	00:05:16:20:47:51.93	10.10	41.23	10	4.4							
13: Fixed Depth	00:05:16:20:47:51.27	10.17	41.95	7+	4.4	6	166	1.72	0.49	-120	1.25	3.45
14: Traveltimes	01:04:06:16:36:30.99	11.403	39.659	62	3.6	23	82	2.06	2.10	-51	0.72	4.97
14: Fixed Depth	01:04:06:16:36:29.10	11.492	39.445	5+	3.6	8	171	1.53	0.7	-51	0.7	0.8
15: Traveltimes	01:05:12:01:44:16.07	9.508	39.691		3.6	11	123	2.32	0.46	-34	0.35	0.86
15: Traveltimes	01:05:12:01:44:14.22	9.541	39.658		3.6	10	84	1.44	0.4	-34	0.4	0.7

D = depth in km. * = depth was determined from regional depth phases (Langston et al., 2002). Otherwise depths were determined from only P and S arrival times. M = magnitude. Magnitudes in this study are based on the ML scale from Langston et al. (1998). ISC magnitudes are a mixture of different types. N = number of stations used in the event location. Gap = azimuth range in stations. RMS = Rms error in arrival times. Smaj, Smin, Sez, Az = dimensions (in kms) and orientation of the error ellipse. For this study, the numbers in the table are for a 68% confidence level. * on Sez numbers indicates that the depth uncertainty was obtained from modeling regional depth phases (Langston et al., 2002).

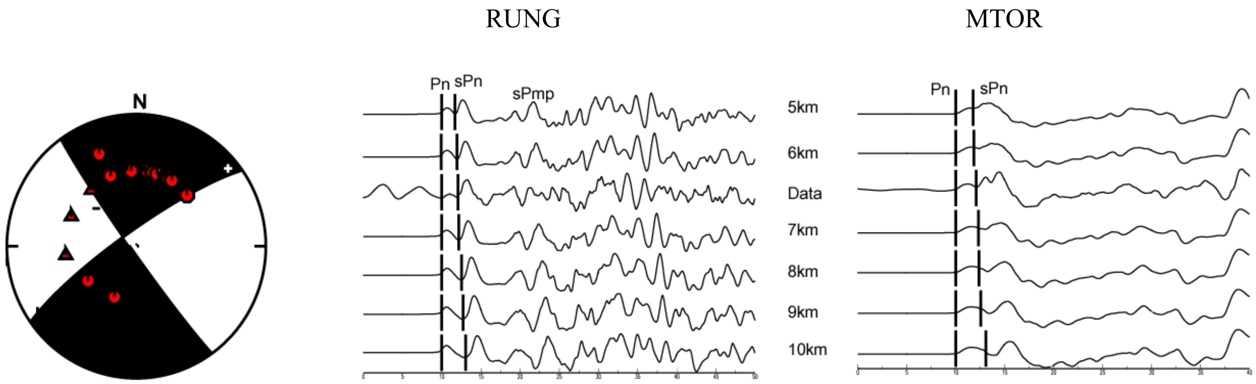

Figure 2. Waveforms and focal mechanisms from the 16 November 1994 Mbeya event (8: in Table 2) recorded at RUNG ($\Delta = 248$ km) and MTOR ($\Delta = 480$ km) and synthetics for source depths between 5-10 km.

TABLE 3. Focal mechanisms for events in Table 2.

	Strike (deg)	Dip (deg)	Rake (deg)
Event 1	301	64	-11
Event 2	335	35	-10
Event 3	345	43	-26
Event 4	318	36	-63
Event 5	335	36	-10
Event 6	204	80	-20
Event 7	303	46	-35
Event 8	143	88	-5
Event 9	93	69	-22
Event 10	215	55	-65
Event 11	162	43	-71
Event 12	316	68	-77
Event 13	105	64	-63
Event 14	54	85	-4
Event 15	3	53	-71

Ongoing Work

In all of these steps it is crucial to have good velocity models for the crust and upper mantle. We are using analyses of receiver functions, surface waves, and seismic refraction profiles to provide independent estimates of crustal and mantle velocities. In addition, we are in the process of making surface wave dispersion measurements of data from the three regional networks in the area. We are measuring both Love and Rayleigh surface wave group velocities using a multiple narrow-band filter technique. Combined with thousands of other measurement made in the broader regional area (Pasyanos et al., 2001), we are conducting a high resolution group velocity tomography of northeastern Africa. Preliminary surface wave tomography results can be seen for eastern Africa in Figure 3 for 20 and 60 second period Rayleigh waves. These maps will be inverted for crustal and upper mantle structure. Using near-regional data will enable us to make more accurate short-period (5-15 seconds) measurements, which will allow us to constrain velocities in the uppermost crust. We will use the surface wave analysis, with receiver functions and other data, to improve the velocity model of the crust and upper mantle, which will in turn improve the event locations.

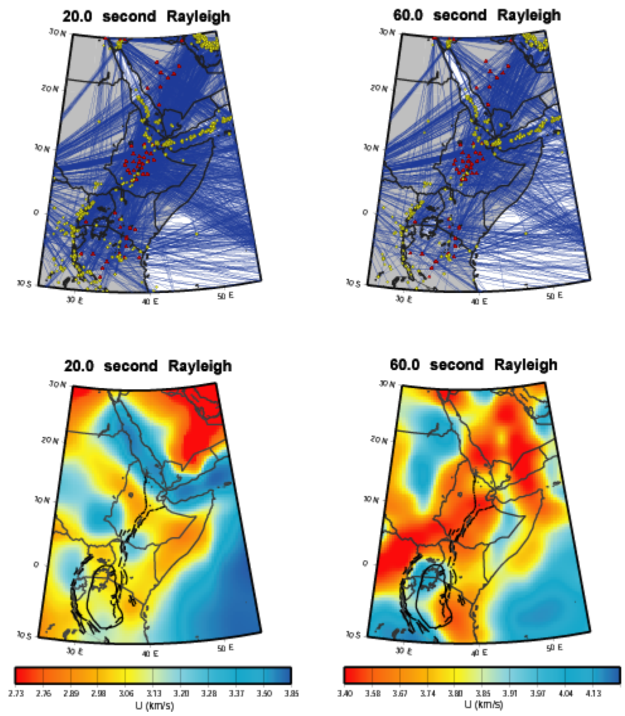

Figure 3. Path locations and preliminary results of the tomography for 20 and 60 second Rayleigh waves

To expand the catalog of events in northeastern Africa, we are taking events located using the approach described above and using them along with teleseismic GT15-25 events (Engdahl, et. al., 1998) as calibration events to construct travel-time correction surfaces using the kriging method of Schultz et al., (1998, 1999) and Myers and Schultz (2000). The travel-time correction surfaces will be used together with local and regional P arrivals to determine epicenters and origin times for numerous other events in the Ethiopia, Kenya, and Tanzania data sets.

The travel-time correction surfaces are constructed following the approach outlined by Myers and Schultz (2000). For the regional networks, we calculate travel-time residuals for the calibration events relative to a regional velocity model, IASPI91 (Kennett et. al. 1991) for the teleseismic events and the Tanzania velocity structure from Table 1 for the regional events. The travel-time residuals will be assigned to the respective calibration epicenter, forming a set of spatially varying travel-time correction points. This set of points will then be declustered to reduce the dimensions of the observations, reducing singularities, and this refined set of calibration points is then modeled with a variogram (variance as a function of spatial separation). The variogram *-----is used with non-stationary Bayesian kriging to form continuous travel-time surface that will provide source-specific corrections for each station in the regional networks. In locating epicenters, a standard location algorithm will be used with the kriging corrections applied. A conservative uncertainty estimate for the kriging correction is used to characterize the travel-time-prediction error, according to the procedure followed by Myers and Schultz (2000). This conservative estimate will be developed using rigorous statistical modeling with available seismic data. Cross-validations will be provided to ensure that the estimates are accurate. In general, these statistics will be used as input to generate chi-squared distribution for robustly determining the final reference event error ellipses.

Preliminary P –wave results for station BGCA can be seen in Figure 4. P and S correction surfaces are being developed for stations DBIC, BOSA, LBTB, and TAM.

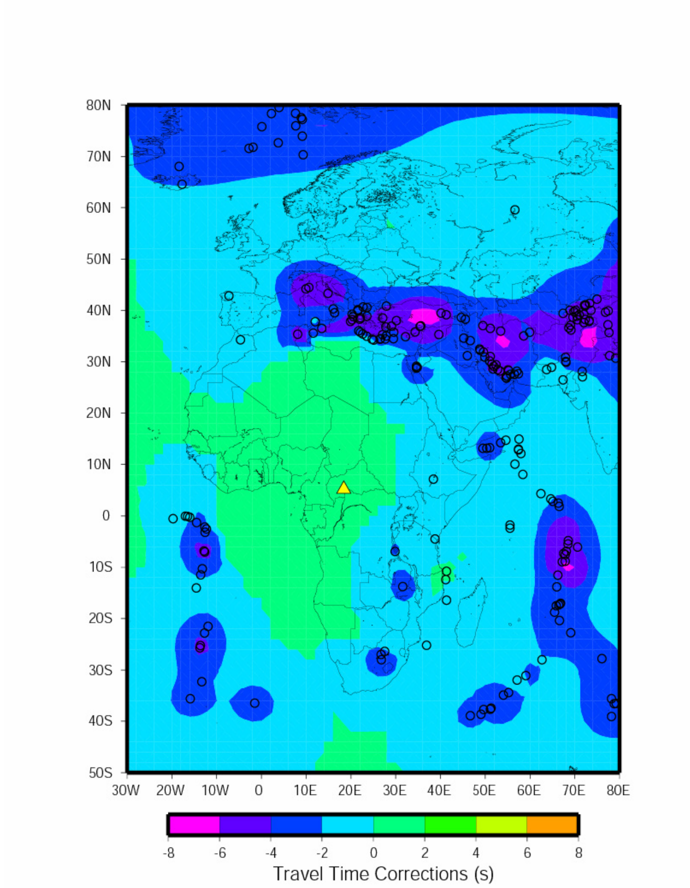

Figure 4. P wave traveltime correction surface for BGCA in the Central African Republic.

Future work will focus on obtaining accurate hypocenters for many additional regionally recorded events in Ethiopia. Figure 5 shows the distribution of events recorded in Ethiopia between April 2000 and March 2002. Accurate locations will be obtained for many of these events with M>3.5 using a combination of the modeling techniques discussed above.

CONCLUSIONS

Accurate event locations for fourteen M>3.5 events in northeastern Africa have been obtained so far using data from the Tanzania Broadband Seismic Experiment and the Ethiopia Broadband Seismic Experiment. Focal mechanisms for most of these events have been obtained by modeling P and SH polarities and amplitude ratios in a grid search method. Epicenters have been constrained by using P and S arrival times. Focal depths have been constrained by waveform modeling of regional and local depth phases. Most of the earthquakes occur on either the western or eastern branch of the East African Rift System, and the mechanisms obtained are all normal or strike-slip. Preliminary epicentral locations for several hundred additional local and near-regional earthquakes have been obtained for Ethiopia using P arrival times.

The Bayesian kriging method is being used with the well located events to construct regional travel-time correction surfaces for northern Africa. To improve further our capabilities to accurately locate events in this part of the world, we are also using surface wave data to construct new velocity models of the crust and upper mantle. Group velocity measurements from many thousand station event pairs ranging from 15-60 second periods for Rayleigh and Love waves have been measured, and these measurements have been inverted to produce group velocity maps of eastern Africa.

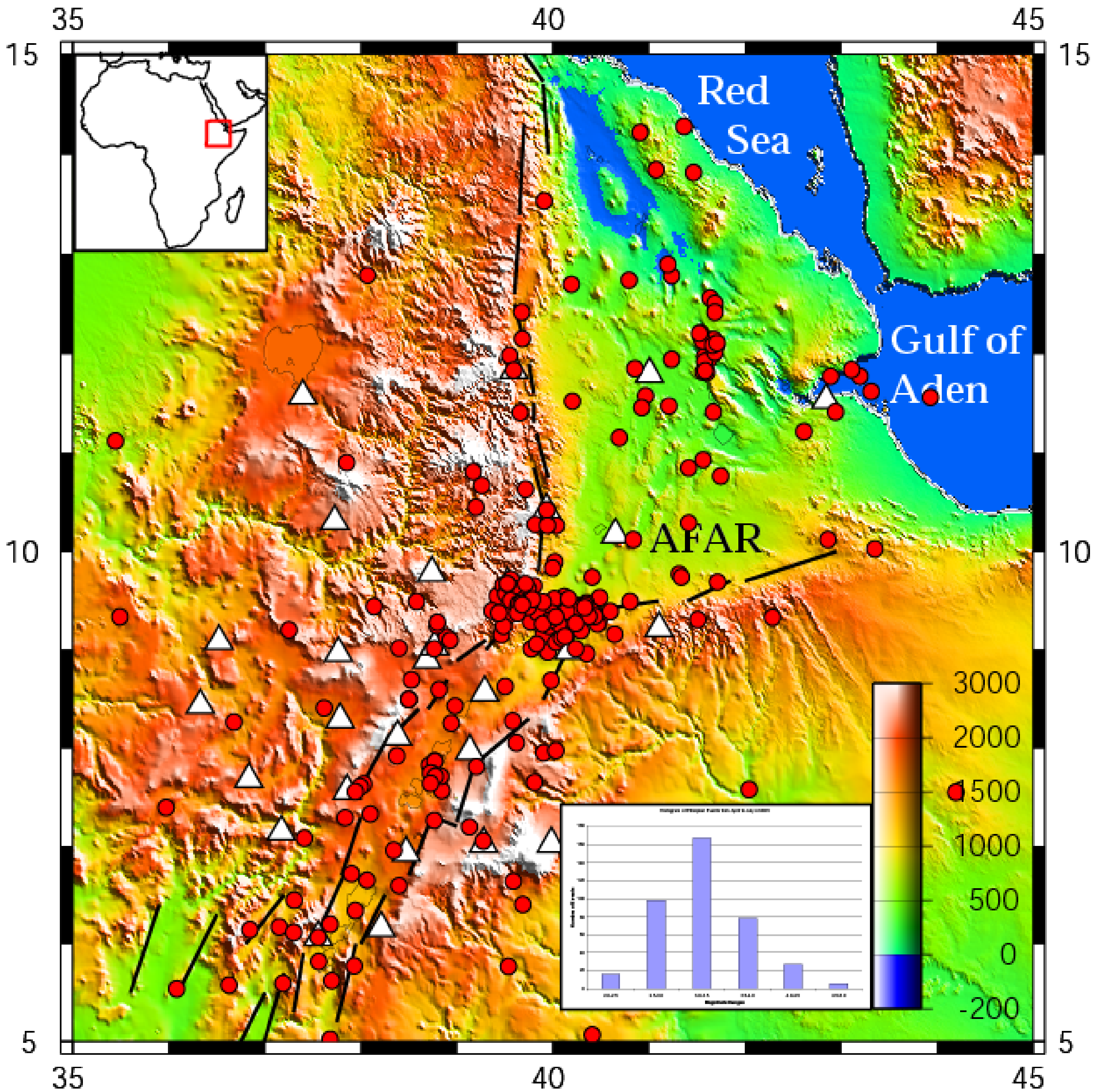

Figure 5. Seismicity (red circles) in Ethiopia with M > 2 from April 2000 to March 2002. Inset histogram of magnitude of events (20 + events M > 4). Seismic stations are shown by white triangles.

REFERENCES

Brazier, R., A.A. Nyblade, C. A. Langston, and T.J. Owens, Pn velocities beneath the Tanzania Craton and adjacent rifted mobile belts, East Africa, *Geophys. Res. Lett.,* 27, 2365-2368, 2000.

Engdahl, E. R., R. D. Van der Hilst and R.P. Buland, Global teleseismic earthquake relocation with improved travel times and procedures for depth determination. *Bull. Seis. Soc. Am., 88*, 722-743, 1998.

Fuchs, K., Altherr, B., Muller, B., and Prodehl, C., Structure and dynamic processes in the lithosphere of the Afro-Arabian rift system: *Tectonophysics, 278*, 1-352, 1997.

Kennett, B.N.L., and E. R. Engdahl, Travel Times for global earthquake location and phase identification, *Geophys. J. Int. ,* 105, 429-465, 1991.

Kennett, B.N.L., Seismic wave propagation in stratified media, *Cambridge University Press*, 1983.

Lahr, J.C., Hypoellipse, a computer program for determining local earthquake hypocentral parameters, magnitude and first motion pattern, U.S. Geological Survey Open File Report 89-116, 1993.

Langston, C.A., R. Brazier, A.A. Nyblade and T. J. Owens, Local magnitude scale and seismicity rate for Tanzania, East Africa, *Bull. Seis. Soc. Am., 88,* 712-721, 1998.

Langston, C.A., A.A. Nyblade, and T.J. Owens, Regional wave propagation in Tanzania, East Africa, *J. Geophys. Res.,* 107, 10.1029, 2002.

Last, R., A.A. Nyblade, C.A. Langston, and T.J. Owens, Crustal structure of the East African plateau from receiver functions and Rayleigh wave phase velocities, *J. Geophys. Res., 102,* 24469-24483, 1997.

Myers, S., and C. Schultz, Improving sparse network seismic location with Bayesian kriging and teleseismically constrained calibration events, *Bull. Seis. Soc. Am., 90*, 199-211, 2000.

Nyblade, A.A., C. Birt, C. A. Langston, T.J. Owens, and R. J. Last, Seismic experiment reveals rifting of craton in Tanzania, *Eos Trans. AGU, 77,* 517-521, 1996.

Nyblade, A.A., Crust and upper mantle structure in East Africa and the origin of Cenozoic extension, magmatism and plateau uplift, in *Magmatic Rifted Margins*, edited by M. Menzies, C. Ebinger and S. Klemperer, Geological Society of America special paper 362-0, in press, 2002.

Pasyanos, M.E., W.R. Walter, and S.E. Hazler, A surface wave dispersion study of the Middle East and North for monitoring the Comprehensive Nuclear-Test-Ban Treaty, *Pure and Applied Geophysics*, 2001.

Schultz, C., S. Myers, J. Hipp, and C. Young, Nonstationary Bayesian kriging: a predictive technique to generate spatial corrections for seismic detection, location and identification, *Phys. Earth. Planet. Int., 113*, 321-338, 1999.

Schultz, C., S. Myers, J. Hipp, and C. Young, Nonstationary Bayesian kriging: a predictive technique to generate spatial corrections for seismic detection, location and identification, *Bull. Seis. Soc. Am., 88,* 1275-1288, 1998.

Snoke, J.A., Munsey, J W; Teague, Alan G; Bollinger, G A. A program for focal mechanism determination by combined use of polarity and SV-P amplitude ratio data, *Seismological Society of America, Eastern Section, 56th annual meeting, Earthquake Notes, vol.55, no.3, pp.15, Sep* 1984.